

Supplementary Information for

Unraveling the stochastic transition mechanism

between oscillation states by landscape and minimum

action path theory

Jintong Lang, Chunhe Li

Chunhe Li.

E-mail: chunheli@fudan.edu.cn

This PDF file includes:

Supplementary text

Figs. S1 to S15

Table S1

Supporting Information Text

The path score of the two-dimensional model. Here we define θ_d as the difference between the barrier angle and the escape angle. Through a small amount of CLE simulation, we obtain the mean and variance of θ_d . Thus, we can predict most probable transition path through the path score. As is shown in Figure S8, we calculate the path score of the transition path in two dimensional model. Take $\omega = 75$ as an example, we test the case of $\theta_d = 20 - 50$, and determine that the escape angle of the highest score is about 280 and the barrier angle of the highest score is about 300, which is in accordance with the result in Figure 3. Furthermore, when θ_d is in a small certain range, the maximum value of path score is stable. So we can estimate θ_d through a few simulations by CLE and calculate the accurate path score. These results show that the critical points of the most probable transition path can be directly predicted by combining the results of flux and barrier height.

The distribution of FPT (first passage time) indicates the memoryless of the transition. About the FPT, we are also interested in finding the probability distribution of escape times from the stable limit cycle. Assuming that escape is a rare event focused around a certain point in the cycle, the escape problem can be described as a Bernoulli process with low success probability p taking place every period of the cycle $\tau = 2\pi/\omega$, at times $t_n = 2\pi n/\omega$. The probability of exiting at the n th revolution follows the geometric distribution $P(t_n) = p(1 - p)^{\frac{\omega t_n}{2\pi} - 1}$. Following rare event theory, we can write the success probability as $p = e^{-S\Omega}/C$, obtaining the geometric distribution,

$$P(t_n) = \frac{(1 - e^{-S\Omega}/C)^{\frac{\omega t_n}{2\pi}}}{C e^{S\Omega} - 1} \quad [1]$$

Comparing the distributions Equation (1), with the probability distribution of MFPT obtained over several CLE realizations of the two dimensional model, we obtained a good agreement (Figure S9, S15). This shows that the simulated results accord with geometric distribution, which indicates that the transition between limit cycles is memoryless.

As shown in Figure S15, the revolution of the simulated transition paths by CLE is usually greater than 1 and probably bigger in NF- κ B model. Here we show the simulated transition paths by CLE

with 2-3 revolution in Figure 5E-F for clarity. On the other hand, the revolution of the transition paths calculated by MAP theory are 1 (Figure 5C) because the action of the transition path will increase with the length of it.

The path score of the NF- κ B model. The path score of the transition path is calculated in NF- κ B model (Figure S13). Here, the variance of θ_d is large because the barrier height is very low at most positions. We test the case of $\theta_d = 80 - 210$. Here the escape angle of the highest score is about 260, while the barrier angle of the highest score is everywhere, in accordance with the result in Figure 7C, D. Therefore, we can still use the method above to estimate the critical points of the trajectory in the actual biological model.

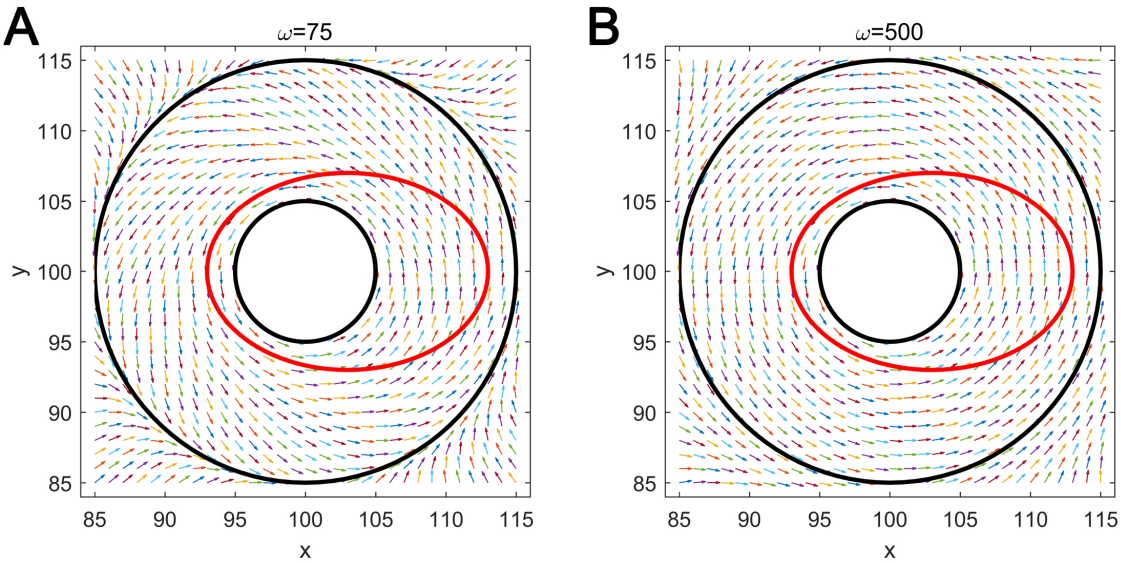


Fig. S1. The vector field of the dynamic system. Two black circles represent two limit cycles $r = c$ and $r = d$ respectively, and the red ellipse represents the ellipse for $E = 0$. ω is set to be 75 (A) and 500 (B) individually. Other parameters are the same as the ones in Figure 1.

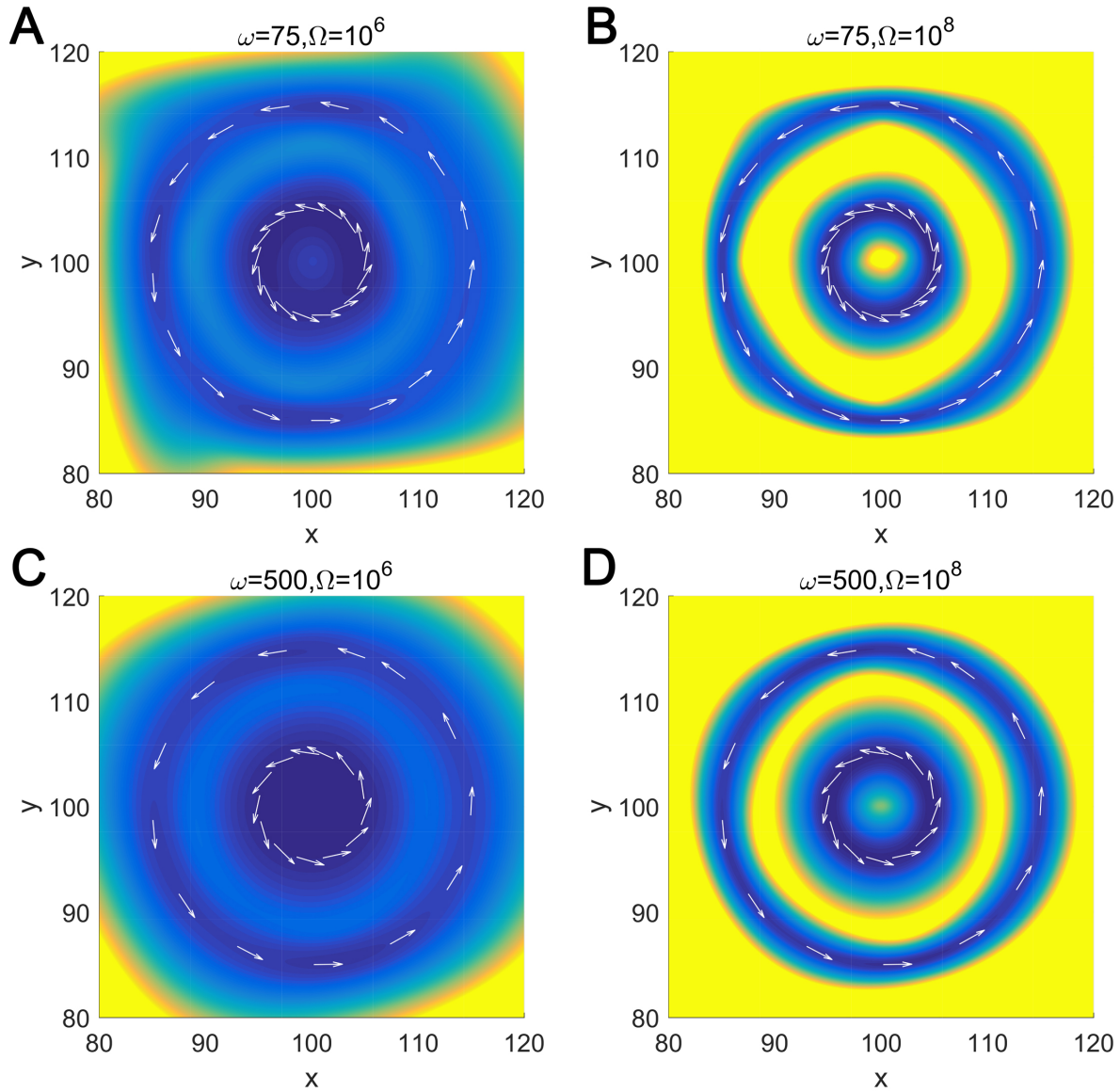


Fig. S2. Comparison of the potential landscape for two-dimensional model at different ω and Ω . The landscape is characterized by different colors, where the blue region represents lower potential or higher probability, and the yellow region represents higher potential or lower probability. The outer loop and the inner loop correspond to two stable limit cycles ($r = c$ and $r = d$) with different oscillation periods, respectively. The white arrows represent probabilistic flux. Other parameters are the same as the ones in Figure 1.

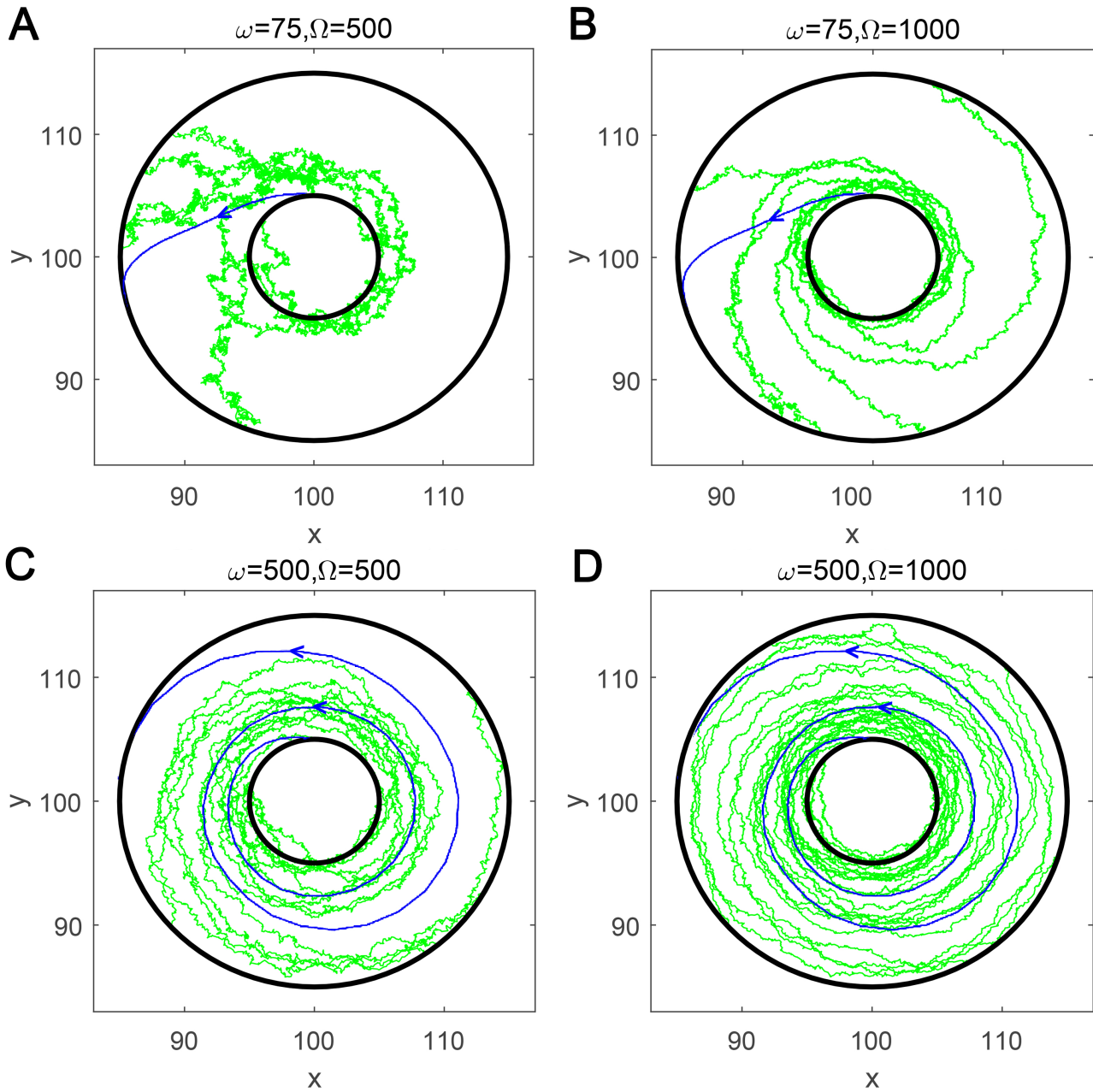


Fig. S3. Comparison of the transition path from the inner cycle to the outer cycle in the two-dimensional model. Results show 5 trajectories of the CLE (green) compared with the MAP (blue). We only show the last part of the CLE trajectories for the sake of clarity. ω is 75 (A-B) and 500 (C-D) respectively. Ω is set to be 500 (A and C) and 1000 (B and D) respectively. Other parameters are the same as the ones in Figure 1.

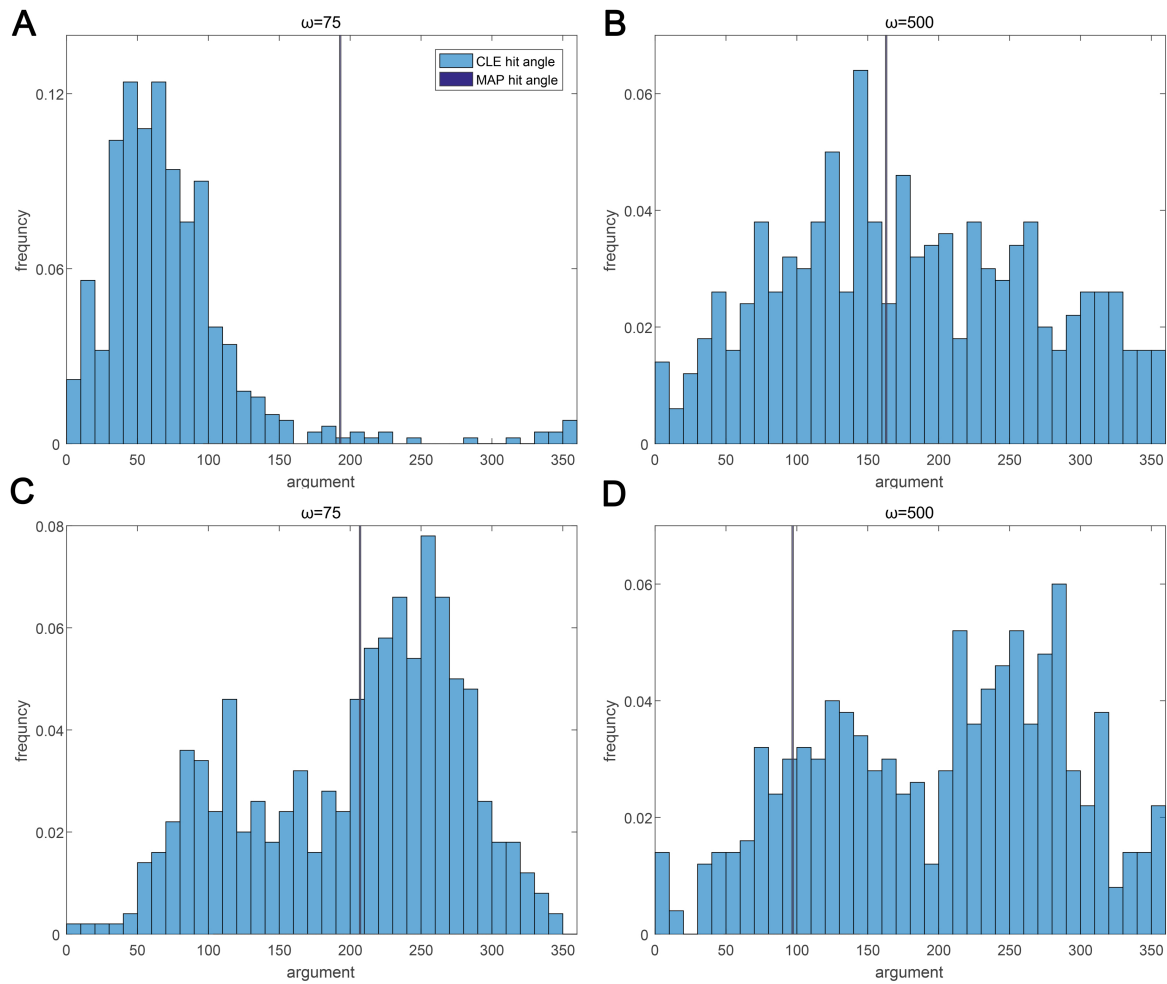


Fig. S4. Comparison of the hit angle distribution (blue) with the hit angle predicted by the MAP (dark blue) in the two-dimensional model. (A-B) The paths from the outer cycle to the inner cycle for $\omega = 75$ (A) and $\omega = 500$ (B). (C-D) The paths from the inner cycle to the outer cycle for $\omega = 75$ (C) and $\omega = 500$ (D). Here the volume parameter (Ω) is 500. Other parameters are the same as the ones in Figure 1.

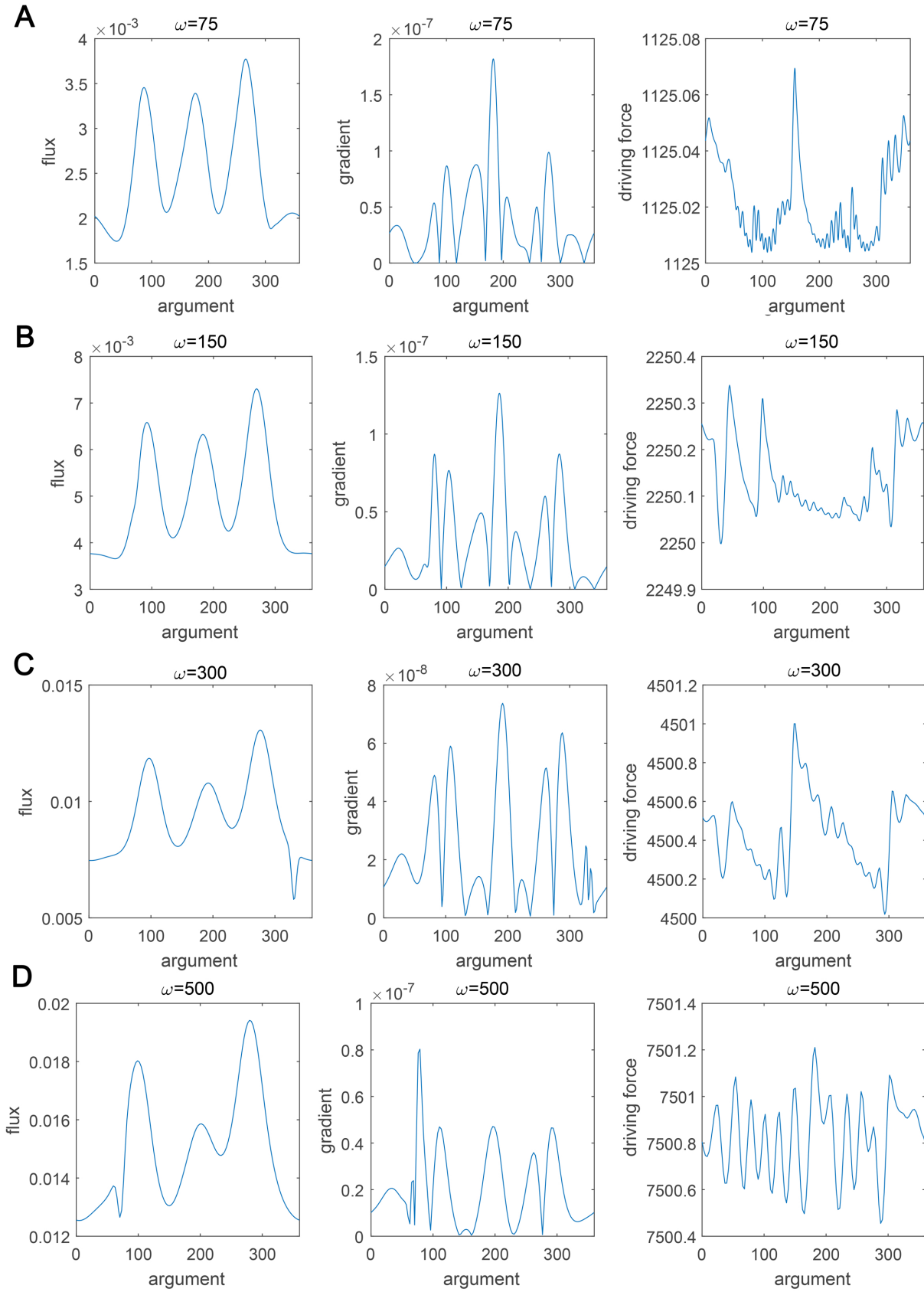


Fig. S5. Comparison of the flux, gradient and driving force on the outer cycle in the two-dimensional model for $\omega = 75$ (A), $\omega = 150$ (B), $\omega = 300$ (C) and $\omega = 500$ (D). Here the volume parameter (Ω) is 10^7 . Other parameters are the same as the ones in Figure 1.

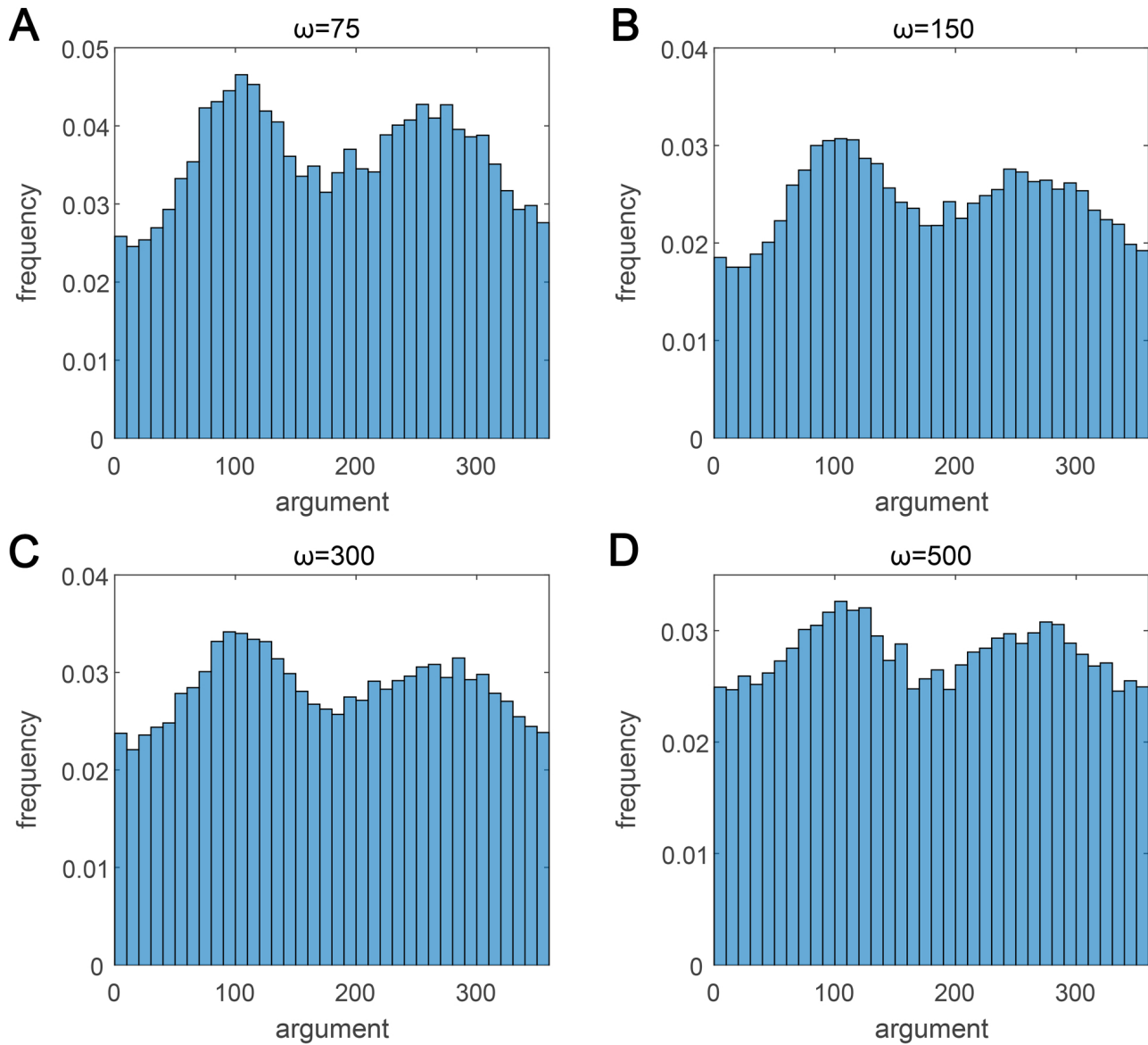


Fig. S6. The distribution of try-to-escape angle of the paths from outer cycle to inner cycle in the two-dimensional model for $\omega = 75$ (A), $\omega = 150$ (B), $\omega = 300$ (C) and $\omega = 500$ (D). Here the volume parameter (Ω) is 0.003. Other parameters are the same as the ones in Figure 1.

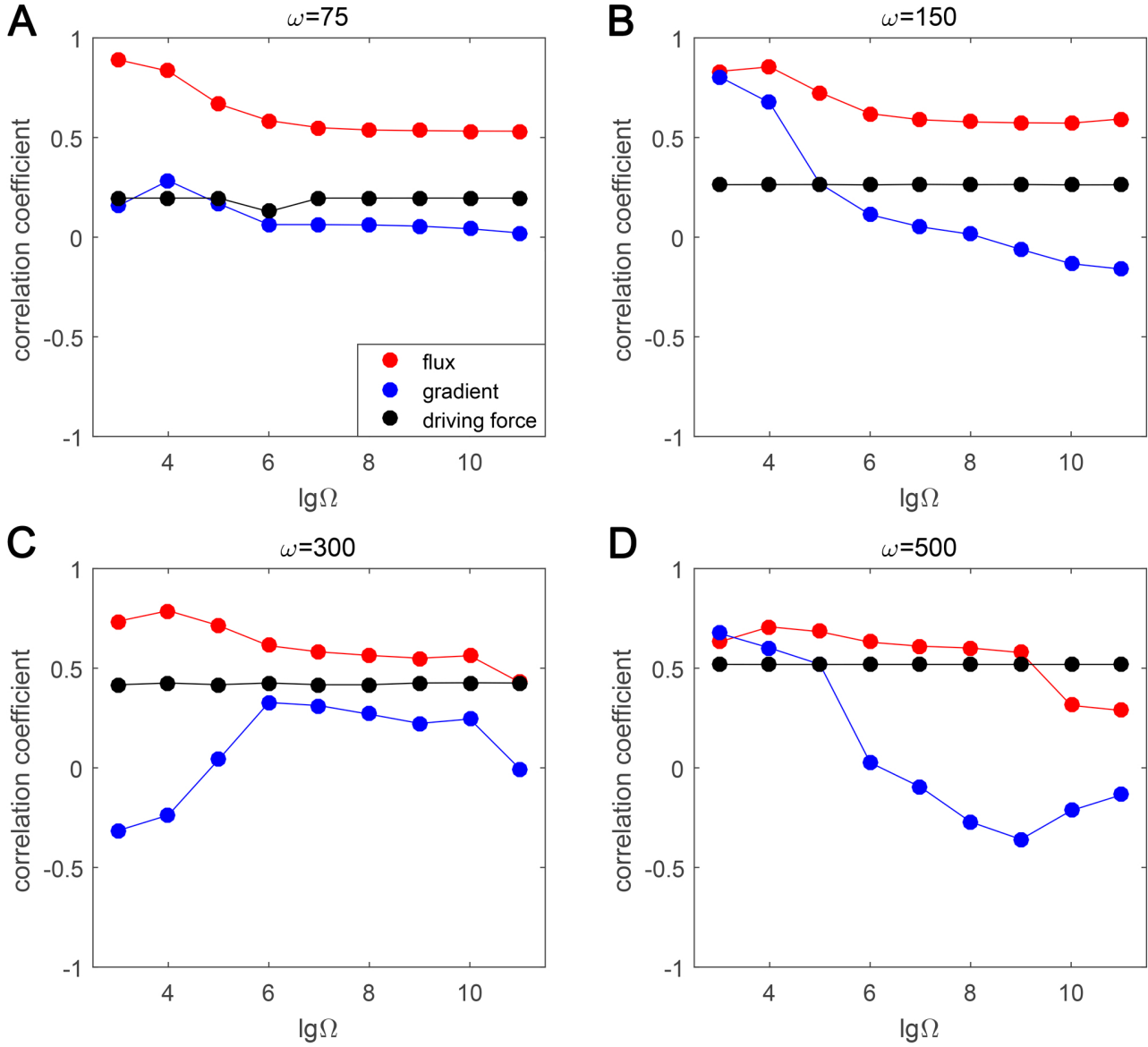


Fig. S7. The correlation coefficient between flux and try-to-escape angle (red), between gradient and try-to-escape angle (blue), between driving force and try-to-escape angle (black) in the two-dimensional model for $\omega = 75$ (A), $\omega = 150$ (B), $\omega = 300$ (C) and $\omega = 500$ (D). Other parameters are the same as the ones in Figure 1. We can see that the flux has good correlation with try-to-escape angle across different Ω .

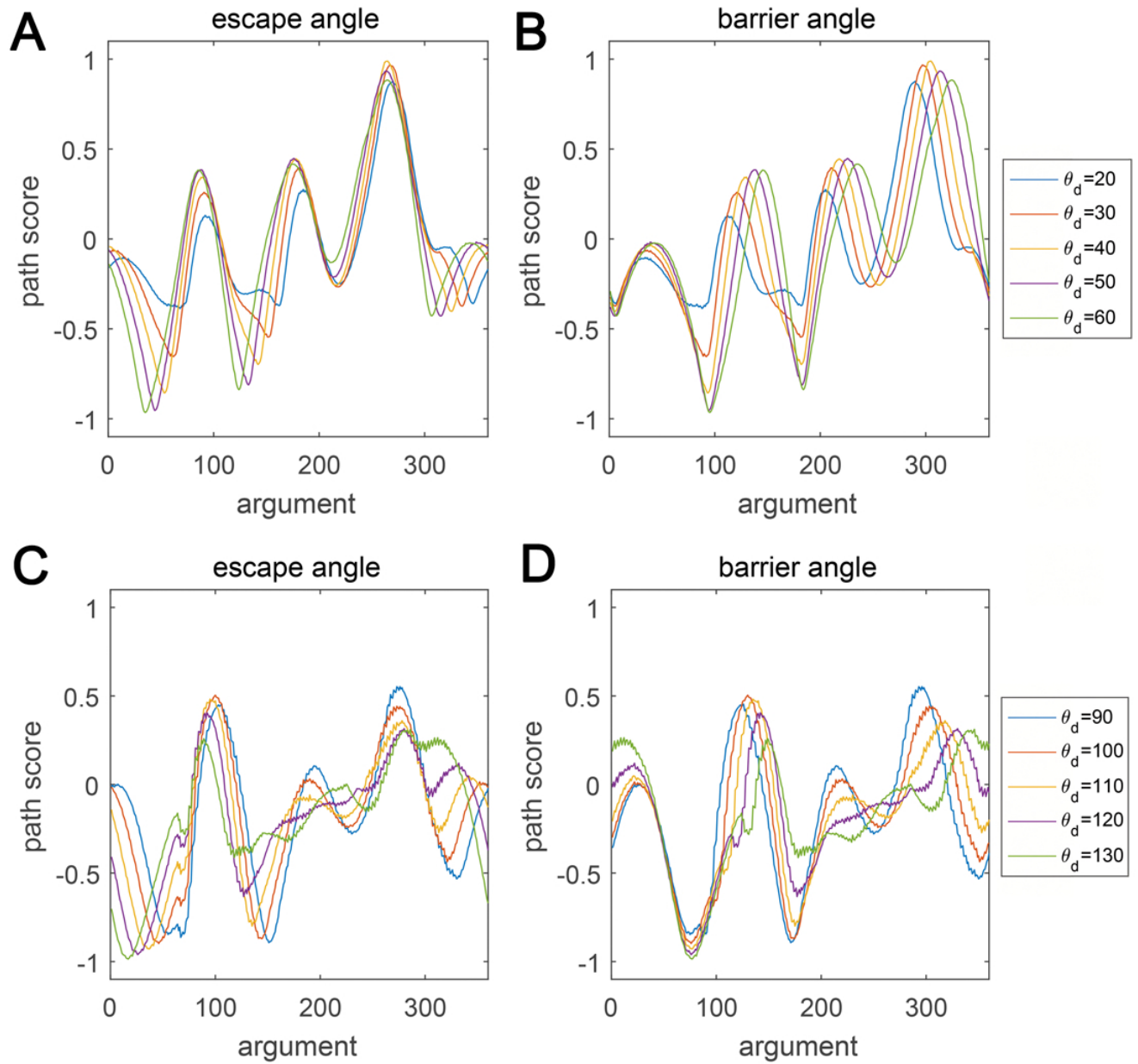


Fig. S8. The path score of the two-dimensional model on escape angle (A and C) or barrier angle (B and D) for $\omega = 75$ (A-B) and $\omega = 500$ (C-D).

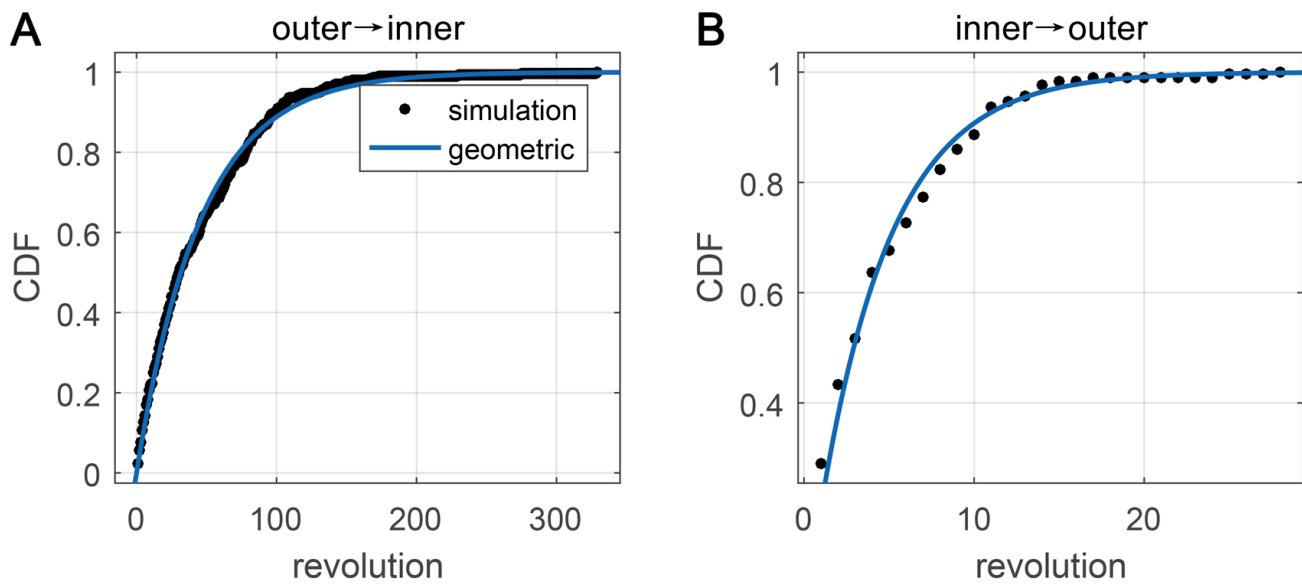


Fig. S9. Comparison of the cumulative distribution function (CDF) of the number of turns for 300 realizations of the two-dimensional model with $\omega = 75$. Here the volume parameter (Ω) is 500. Other parameters are the same as the ones in Figure 1. (A) The path is from the outer cycle to the inner cycle. (B) The path is from the inner cycle to the outer cycle.

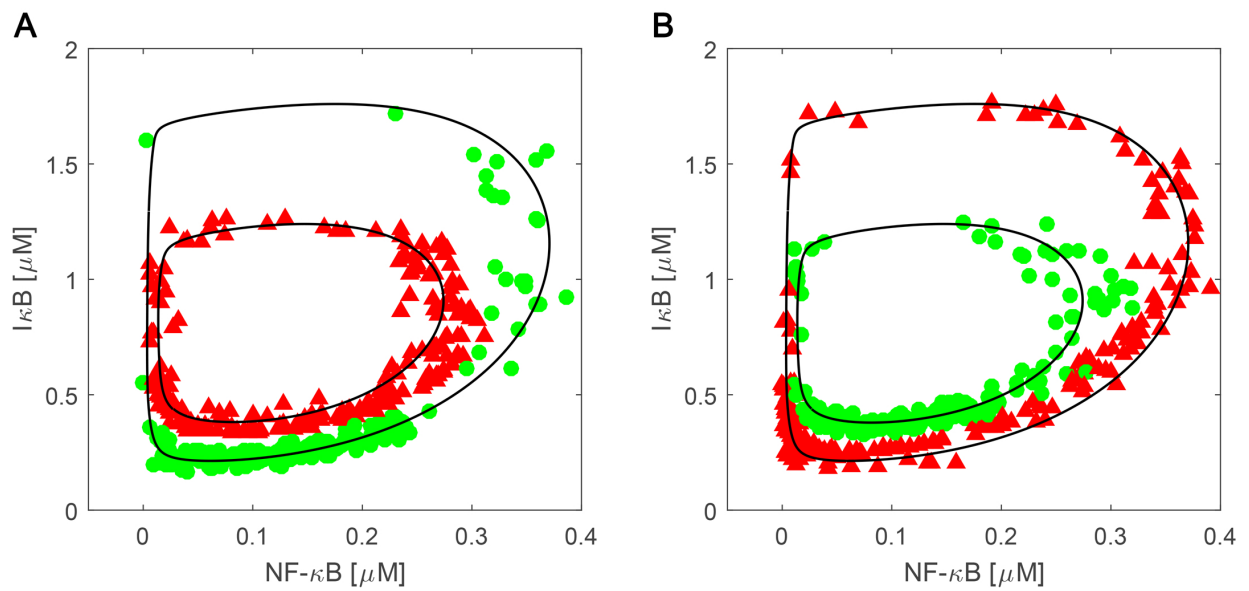


Fig. S10. The statistic of the escape locations of the inner limit cycle and the hit locations of the outer limit cycle in the NF- κ B model from 200 simulations. Here the volume parameter (Ω) of the transition path is 500. Green points represent escape locations, and red points represent hit locations. (A) The path is from the outer cycle to the inner cycle. (B) The path is from the inner cycle to the outer cycle.

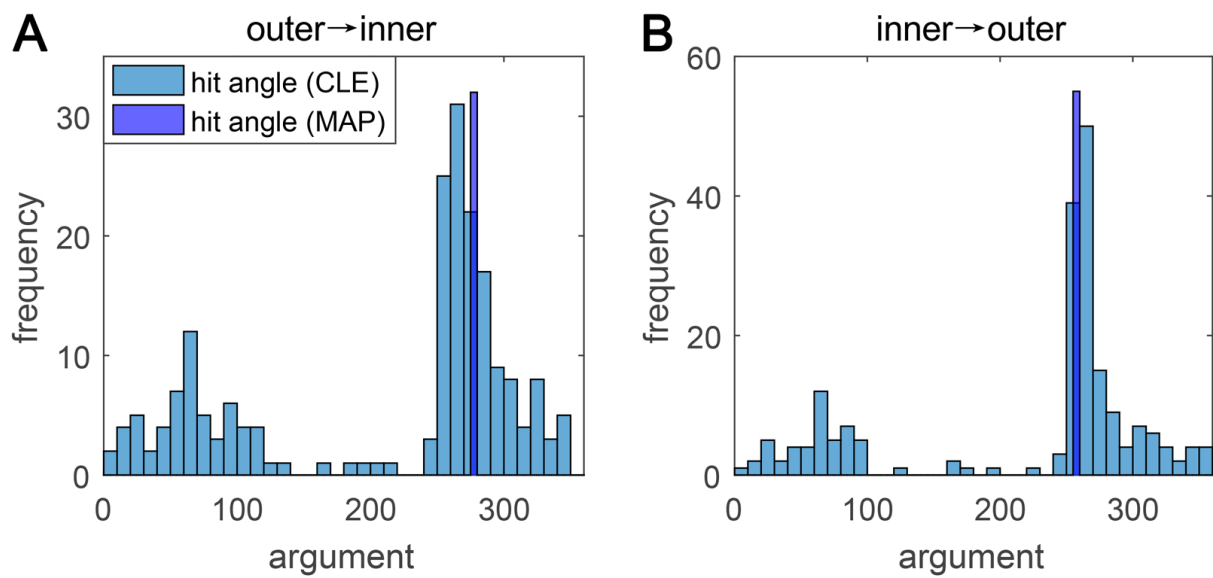


Fig. S11. Comparison of the hit angle distribution (blue) with the hit angle predicted by the MAP (grey) in the NF- κ B model. (A) The paths from the outer cycle to the inner cycle. (B) The paths from the inner cycle to the outer cycle. Here the volume parameter (Ω) is 500. Other parameters are the same as the ones in Figure 5.

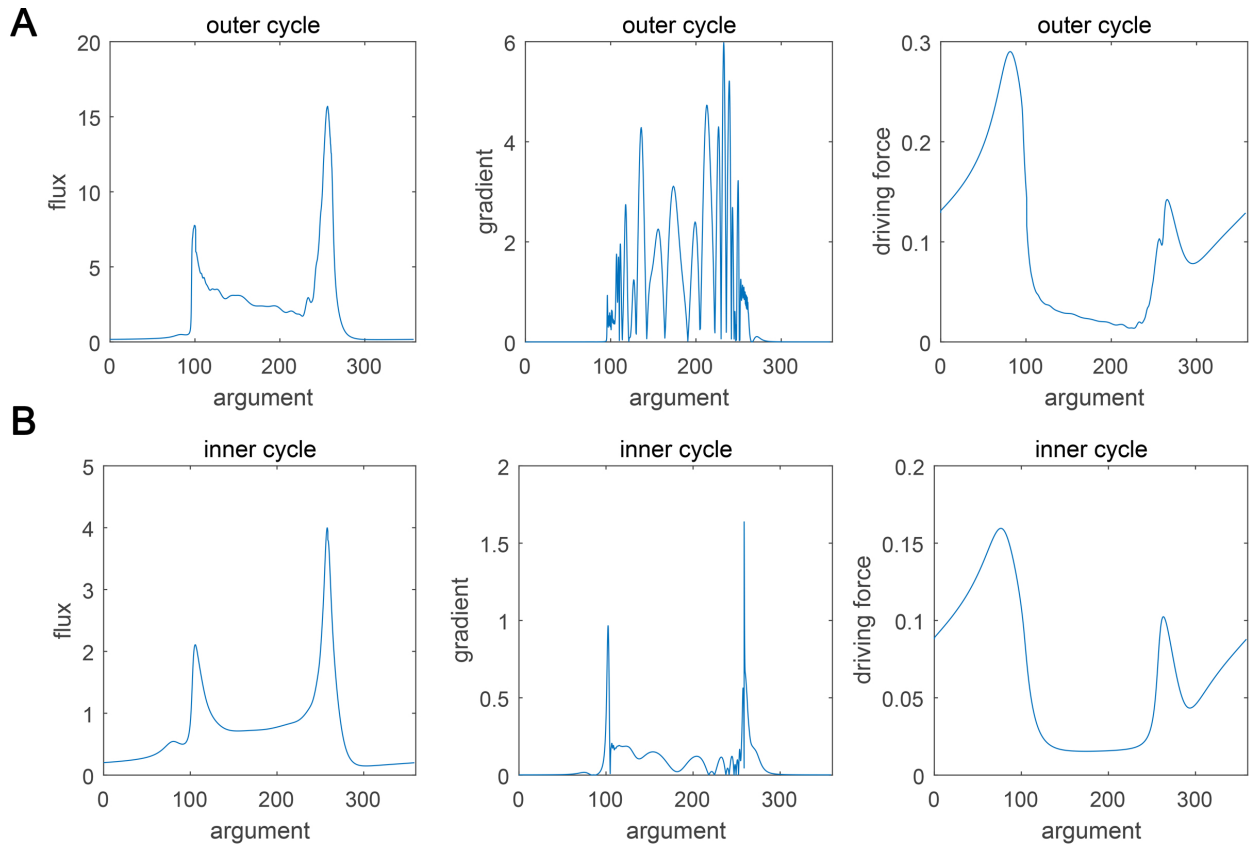


Fig. S12. Comparison of the flux, gradient and driving force on the outer (A) or inner cycle (B) in the NF- κ B model. Here the volume parameter (Ω) is 5×10^7 . Other parameters are the same as the ones in Figure 5.

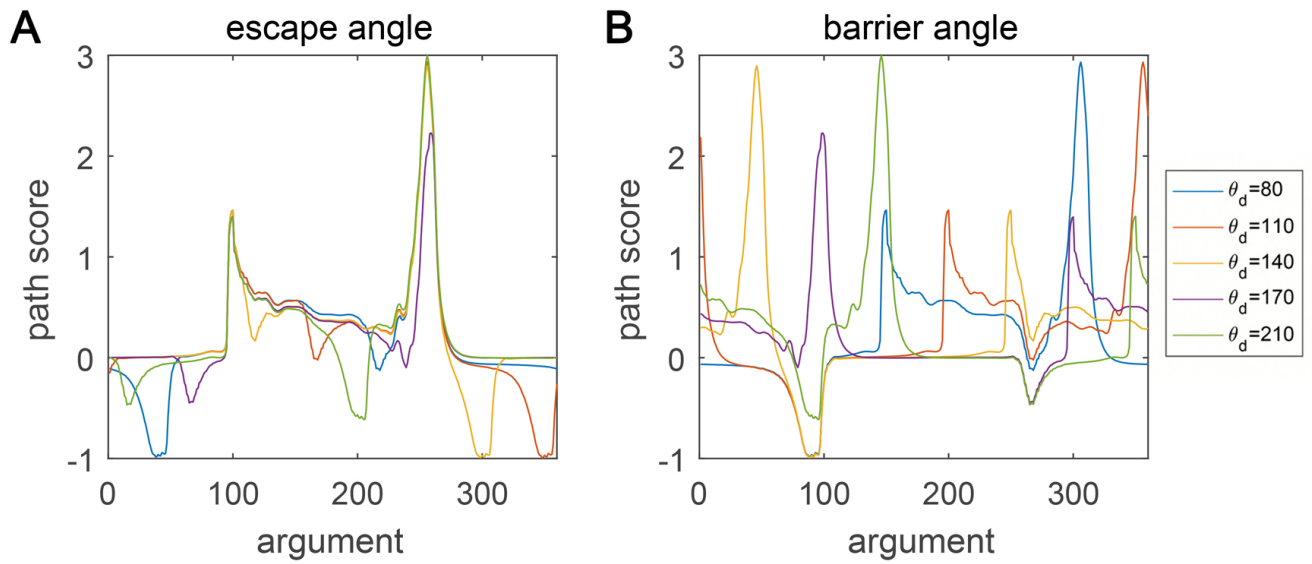


Fig. S13. The path score of NF- κ B model on escape angle (A) or barrier angle (B) for different θ_d in the NF- κ B model. Here the transition path is from outer cycle to inner cycle.

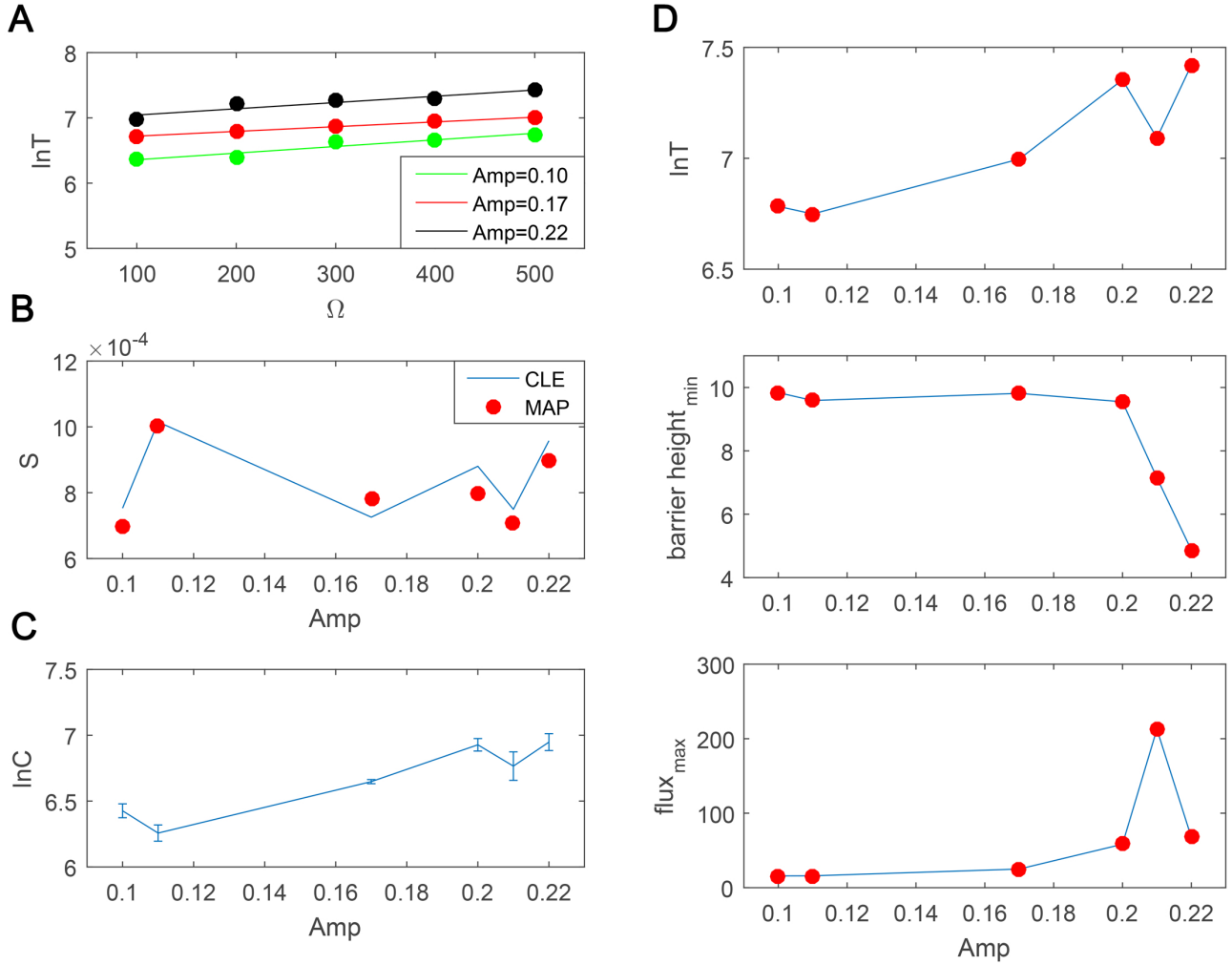


Fig. S14. The estimation of the mean first passage time (MFPT) for the NF- κ B model. (A) Comparison of MFPTs calculated from CLE simulations (lines) with the exponential dependence of the MFPT on Ω given by S (red points). The linear relationship between $\ln T$ and Ω is good. (B-C) Based on the formula $\ln T \approx \Omega S + \ln C$, the minimal action S and prefactor C can be calculated by CLE (blue line). Meanwhile, we can minimize the action S for different ω by MAP theory (red point). Following the same procedure, the values of the action S are compared for different values of ω . Error bars are standard error of the mean from the CLE. (D) The influence of barrier height and flux on MFPT. Here $\Omega = 500$ for calculating the transition path, and $\Omega = 5 \times 10^7$ for calculating the landscape. (Top) $\ln T$ under different Amp , where T represents MFPT. (Medium) The minimum of the barrier height under different Amp . (Bottom) The maximum of the flux under different Amp .

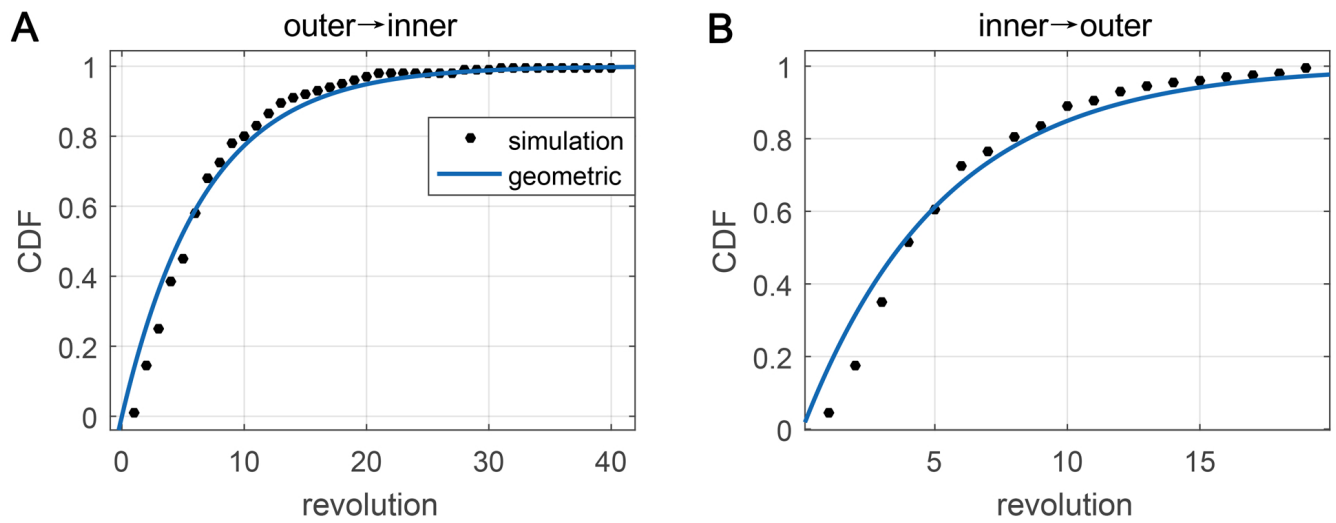


Fig. S15. Comparison of the cumulative distribution function (CDF) of the number of turns for 300 realizations of the mode-hopping model. Here the volume parameter (Ω) is 500. Other parameters are the same as the ones in Figure 5. (A) The path is from the outer cycle to the inner cycle. (B) The path is from the inner cycle to the outer cycle.

Table S1. Parameters of the NF- κ B model.

Parameters	Default value
K_{Nin}	5.4 min^{-1}
K_{lin}	0.018 min^{-1}
k_t	$1.03 (\mu\text{M}) \text{ min}^{-1}$
k_{tl}	0.24 min^{-1}
K_I	$0.035 \mu\text{M}$
K_N	$0.029 \mu\text{M}$
γ_m	0.018 min^{-1}
α	$1.05 (\mu\text{M}) \text{ min}^{-1}$
N_{tot}	$1.0 \mu\text{M}$
k_a	0.24 min^{-1}
k_i	0.18 min^{-1}
k_p	0.036 min^{-1}
k_{A20}	$0.0018 \mu\text{M}$
$[IKK]_{tot}$	$2.0 \mu\text{M}$
$[A20]$	$0.0026 \mu\text{M}$